mathematics

MDPI

Article

An Improvement of Model Predictive for Aircraft Longitudinal Flight Control Based on Intelligent Technique

Mohamed El-Sayed M. Essa [1,*], Mahmoud Elsisi [2,3,*], Mohamed Saleh Elsayed [4], Mohamed Fawzy Ahmed [5] and Ahmed M. Elshafeey [6]

1 Electrical Power and Machines Department, Institute of Aviation Engineering and Technology (I.A.E.T), Egyptian Aviation Academy, Imbab Airport, Giza 12815, Egypt
2 Department of Electrical Engineering, National Kaohsiung University of Science and Technology, Kaohsiung City 807618, Taiwan
3 Department of Electrical Engineering, Faculty of Engineering (Shoubra), Benha University, 108 Shoubra St., B.O. Box 11629, Cairo 13511, Egypt
4 Aeronautical Engineering Department, Faculty of Engineering, Zagazig University, Zagazig 44519, Egypt
5 Electrical Engineering Department (Control Engineering), Faculty of Engineering, Modern University for Technology & Information, Cairo 4410240, Egypt
6 Electronics and Communication Department, Institute of Aviation Engineering and Technology (I.A.E.T), Egyptian Aviation Academy, Imbab Airport, Giza 12815, Egypt
* Correspondence: mohamed.essa@iaet.edu.eg (M.E.-S.M.E.); mahmoud.elsisi@mail.ntust.edu.tw or ahmoudelsisi@nkust.edu.tw (M.E.)

Abstract: This paper introduces a new intelligent tuning for the model predictive control (MPC) based on an effective intelligent algorithm named the bat-inspired algorithm (BIA) for the aircraft longitudinal flight. The tuning of MPC horizon parameters represents the main challenge to adjust the system performance. So, the BIA algorithm is intended to overcome the tuning issue of MPC parameters due to conventional methods, such as trial and error or designer experience. The BIA is adopted to explore the best parameters of MPC based on the minimization of various time domain objective functions. The suggested aircraft model takes into account the aircraft dynamics and constraints. The nonlinear dynamics of aircraft, gust disturbance, parameters uncertainty and environment variations are considered the main issues against the control of aircraft to provide a good flight performance. The nonlinear autoregressive moving average (NARMA-L2) controller and proportional integral (PI) controller are suggested for aircraft control in order to evaluate the effectiveness of the proposed MPC based on BIA. The proposed MPC based on BIA and suggested controllers are evaluated against various criteria and functions to prove the effectiveness of MPC based on BIA. The results confirm that the accomplishment of the suggested BIA-based MPC is outstanding to the NARMA-L2 and traditional PI controllers according to the cross-correlation criteria, integral time absolute error (ITAE), system overshoot, response settling time, and system robustness.

Keywords: robotics and intelligent systems; flight mechanics; model predictive control; bat inspired algorithm; NARMA-L2 controller; pilot stick

MSC: 65K99; 90C99

Citation: Essa, M.E.-S.M.; Elsisi, M.; Saleh Elsayed, M.; Fawzy Ahmed, M.; Elshafeey, A.M. An Improvement of Model Predictive for Aircraft Longitudinal Flight Control Based on Intelligent Technique. *Mathematics* **2022**, *10*, 3510. https://doi.org/10.3390/math10193510

Academic Editors: Denis N. Sidorov and Pantelis Sopasakis

Received: 7 August 2022
Accepted: 18 September 2022
Published: 26 September 2022

1. Introduction

The adjustment of the direction and altitude of an aircraft with less error during the aircraft flight represents the main target of flight control. The objective of control design in the process of flight dynamics is to adjust the direction of the vehicle about its center of gravity (CoG) [1]. The definition of flight dynamics is summarized as the science of the direction of air vehicles and the task of control around defined three dimensions called pitch control, roll control, and yaw control. Additionally, flight systems control is divided

into two categoriesnamed the primary phase and secondary phase control [2]. The primary phase control is utilized for elevators, rudders, and ailerons and it is established to create a safe aircraft flight control. However, the primary control can lead to rotation of the aircraft around the rotational axis. So, secondary phase flight control is utilized to enhance the aircraft's performance characteristics and handle the overloading. The secondary type contains the devices of high lift. Moreover, the control system in an aircraft comprises surfaces of control. In the condition of a deviation in the surface of control, the control designed system will produce a moment about the CoG. Consequently, the aircraft will present a motion in pitch, roll, and yaw. Thus, in the condition of a force applied at a space aft or forward to the CoG, a moment of pitching will be generated which creates pitching of aircraft up or down [3].

In the literature, a lot of control techniques have been applied to solve the above-mentioned control issue of aircraft [4–7].A comparative study between classical and modern control strategies for pitch control of an aircraft system is presented in [8]. Furthermore, the longitudinal motion of a rigid plane is represented by nonlinear differential equations that are developed from Newton's second law of motion. In addition, completed work for characteristics of flight, and mathematical models based on flight mode and type of unmanned aerial vehicle (UAV) for an aircraft are given in [9]. However, these equations have been linearized using a small disturbance theory. In [10], a Proportional-Integral-Derivative (PID) controller is introduced for General Navion Aircraft by considering its longitudinal motion. In addition, the control design is performed via a MATLAB/programming model, and the angular deflection of the elevator is chosen as a command input and the output is selected to be the pitch angle. However, the introduced PID is simpler and cannot handle system constraints. In [11], a sliding mode control (SMC) is introduced based on the linearization of the aircraft, with the elevator deflection and the pitch angle as the trim variables. While the SMC suffers from a chattering problem that requires special switching in the practical implementation. In [12,13], fuzzy logic control (FLC)is applied for aircraft longitudinal motion based on the Takagi–Sugeno modeling method. The model of Takagi–Sugenofor the aircraft motion along the proposed trajectory is utilized for the designing of a state-space parallel decomposition controller (PDC). The designed control system enhances closed-loop stability. However, the authors utilize the trial and error method to adjust the membership function of the FLC which does not enhance the system performance. An FLC algorithm is described to adapt the gains of the PID controller for the longitudinal motion of aircraft in [14,15]. The hybrid Fuzzy PID controller is introduced to enhance the control performance for longitudinal motion of aircraft dynamics. The implementation of the hybrid Fuzzy PID controller requires a high computation process and high cost. In [16], an artificial neural network (ANN) is applied to construct a mathematical model for an aircraft framework with allowed data for the flight framework. The design of flight control for a UAV by applying a nonlinear autoregressive moving average (NARMA-L2) neural network-based feedback linearization and output redefinition method is discussed in [17]. In addition, the issue of using a neural network algorithm forthe flight control of an aircraft in a longitudinal status of a remotely piloted vehicle is discussed in [18]. The identification approach has been established to structure a mathematical representation for rotorcraft and aircraftvia various engineering strategies that areused, for example, in flight tests as presented in the paper [19]. However, the implementation of ANN faces a lot of challenges due to the unavailability of enough datasets for the training and testing to provide high accuracy.

Recently, the concern about applying MPC has increased significantly. The increasing attention to using MPC is produced by its stability and fast response in the case of nonlinearities, constraints, and uncertainties in parameters rather than traditional linear quadratic regulators (LQR) [20–23]. In [20], an MPC is applied for high precision control of the force in an experimental hydraulic system. In addition, the hardware of EHSS position control based on hybrid PID MPC is discussed in [21]. However, the MPC requires fine tuning for its parameters to provide good performance [24–26]. In [27], the tuning of MPC

parameters is depicted for a mathematical model of a house with system identification and precise control of thermal temperature. The tuning strategy of the MPC has been carried out by the cuckoo search algorithm (CSA) for temperature control.In addition, the MPC design based on CSA for the force control of the hydraulic servo system is demonstrated in [28]. However, the CSA requires a fine selection for a lot of factors to optimize the parameters of the MPC. Moreover, the MPC based on the trial and error tuning method for aircraft control is discussed in [29]. Besides, the design of MPC in [29] did nottake into consideration most aircraft problems, such as gust disturbance, nonlinear dynamics, and parameter perturbations. The trial anderror method is notan accurate method and it is considered a waste of time method.

The bat-inspired algorithm (BIA) is proposed in this article as a recent powerful and intelligent method to handle the tuning issue of the MPC parameters to improve their performance. The BIA is considered one of the efficient algorithms that are applied to tune the parameters of different types of controllers for many practical applications [30–38]. Besides, the BIAhas become the most commonly used algorithm among researchers in different fields. In addition, BIAs haveimportant features, such as dealing with several parameters that are used for initializations wherever parameters with a lower number are utilized as compared with other kinds of algorithms. Moreover, another important advantage of BIA is that the rate of convergences is independent of its used parameters. The bat algorithm requires a few tuning factors to reduce the longitudinal deviation of aircraft motion against the nonlinear dynamics of aircraft, gust disturbance, parameter uncertainty, and environmental variations.

Due to the sensitivity of the aircraft field, it requires that the control design be very accurate with high performance including less settling time, rise time, error, and motion overshoot.In fact, the accurate, simple, and fast tuning of the parameters of aircraft controllers represent the main issue and challenge against the problems that face the aircraft control field. As a result, the choosing of an MPC controller that can solve most of the aircraft problems, such as uncertainty, gust, parameter perturbation, and improving the tuning issue via BIA, will contribute to the sensitive aircraft control field.

The proposed MPC as an efficient controller that can handle the uncertainty, nonlinearities, and perturbation is used foraircraft control challenges. The MPC based on BIA is utilized for controlling the longitudinal motion of aircraft to diminish oscillations with low frequency. The BIA is dedicated to finding the best parameters of MPC based on the decreasing of various time-domain objective functions. Besides, the NARMA-L2-based longitudinal motion of aircraft is introduced to evaluate the performance of the suggested MPC based on BIA. Different test scenarios are performed to confirm the effectiveness of the suggested MPC based on BIA. Besides, the proposed controller is compared with the traditional PI controller and theNARMA-L2 controller using different test signals for the pilot stick. The paper is structured as in Figure 1.The contributions of the paper are concluded as follows,

- Introducing the MPC as an effective controller for adjusting the longitudinal motion of aircraft to overcome the nonlinear aircraft dynamics, gust disturbance, parameters uncertainty, and environmental variations.
- The coefficients of the MPC are tuned via the BIA as an intelligent method rather thantrial and error or designer experience.
- Various time-domain objective functions are utilized for the BIA in order to find the best parameters of MPC.
- The longitudinal motion of aircraft control is carried out based on the NARMA-L2 controller to evaluate the accomplishment of the suggested MPC based on BIA.
- The proposed MPC based on BIA is compared with the traditional PI controller and the NARMA-L2 controller using different test signals for the pilot stick.
- The results affirm that the superiority of aircraft performance based on the proposed BIA-based MPC controller emulated with the NARMA-L2 and traditional PI con-

trollers according to the cross-correlation criteria, integral time absolute error (ITAE), overshoot, settling time, and system robustness.

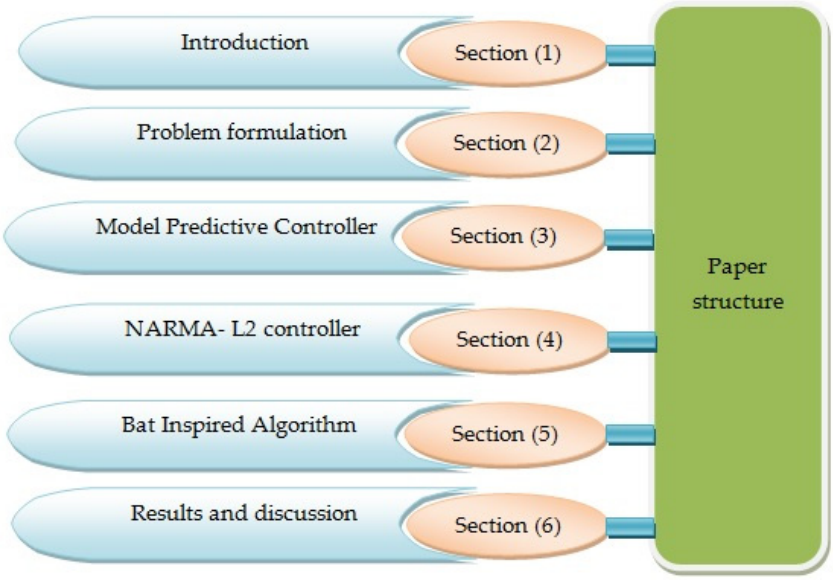

Figure 1. Article structure.

2. Problem Formulation

The accurate aircraft mathematical model is considered as the important first step to analyzingand controlling the aircraft system that may be utilized to handle the control and stability issues. The obtained model modifies the characteristics of flying which are used to control the surfaces and design the flight systems. Newton's second law has been utilized to attain the mathematical equations that manage the behavior of flight vehicle motion.Consequently, the applied forces on aircraft can be demonstrated in mathematic symbols as below in Equation (1) as described in [12–15].

$$\sum F = \frac{d}{dt}(mv) \tag{1}$$

where F refers to force components (F_x, F_y, and F_z) on three-dimensions (x, y, and z), m denotes the mass of the system, v is a representation for velocity sharing both rotational rates (p, q, and r) and linear rates (u, v, and w) in three dimensions (x, y, and z). Furthermore, the parts of force are produced by adding propulsive, aerodynamic, and gravitational forcesaffecting the airplane. The formulation of the moment is depicted in the equation:

$$\sum M = \frac{d}{dt}(H) \tag{2}$$

where, M denotes to instance moment components L, M, and N on the around three dimensions (x, y, and z). In addition, H stands for momentum parts moment as Hx, H_y, and H_z, alongside three dimensions (x, y, and z). The aerodynamic moments and forces are depicted as a function of all variables of motion. Therefore, the equations of motion are introduced as in Equations (3)–(5) [1–3,15].

$$\left[\frac{d}{dt} - X_u\right]u + g_0 cos\theta_0 - X_w w = X_{\delta_e}\delta_e + X_{\delta_T}\delta_T \tag{3}$$

$$-Z_u u + \left[(1 - Z_{\dot{w}})\frac{d}{dt} - Z_w\right]w - \left[u_0 + Z_q\right]q + g_0 sin\theta_0 = Z_{\delta_e}\delta_e + Z_{\delta_T}\delta_T \tag{4}$$

$$-M_u u - \left[(M_{\dot{w}})\frac{d}{dt} - M_w\right]w + \left[\frac{d}{dt} - M_q\right]q = M_{\delta_e} + M_{\delta_T}\delta_T \tag{5}$$

where, X_w, Z_w, M_w and M_w are defined as derivatives of system stability that is determined at the reference flight condition. Additionally, the control factors containing δ_T and δ_e represent the variants from the trim in the thrust or elevator and throttle settings. X_{δ_e}, Z_{δ_e}, M_{δ_e} represent the settings of the X-force, and Z-force parts of the elevator, and the moment due to pitching. The factors X_{δ_T}, Z_{δ_T}, M_{δ_T} stand for the adjustment of the X-force, and Z-force parts of the throttle, and moment due to pitching. X_u and Z_u are a dimensional change of the X-force and Z-force with speed, respectively, while M_u is a dimensional change of pitching moment with speed. M_q and Zq are a dimensional change of pitching moment with pitch rate and dimensional variation of Z-force with pitch rate, respectively. g_0, θ_0 and u_0 are acceleration due to gravity, main rotor collective pitch, and reference value, respectively. The dot symbol over variables of the aircraft system in Equations (3)–(5) are described as the derivative of the variables [14,15].

3. Model Predictive Control Strategy

Advanced control strategies represent the main core in industrial applications that can enhance system performance and improve the rate of industrial production. Among the advanced control strategies, the MPC is a class of effective control methodologies that provides a good performance in different applications [20–27]. In fact, it is a suitable control technique for most industrial application processes because it has the capability of controlling the system within the defined constraints [26]. In addition, it relies on the dynamic models of the industrial process, most linear experimental models are built by using the system identification procedure. In contrast, most field engineers are not well-known the advanced control method in theoretical studies and the relationship between the control decision and the tuning of control system parameters. Consequently, it still has restricted use and implementation in the industrial field [21,28].

Mainly, the computations of the MPC are executed at each sampling time, which can be adjusted by the control designer. These computations depend on the measurements and forecasting of upcoming output values [25]. There are two styles of computations in MPC, the first is set point computations while the second is control computations. The control computations contain the constraints of the process and other parameters that are capable to be manually adjusted.

The control computations depend on the reduction of the forecasted deviations from the command trajectory. The main idea for the operation of MPC strategy and the structure of MPC are given in Figures 2 and 3.

The action of the MPC controller depends on a mathematical representation named cost function (J(k)). The mathematic representation of system constraints and cost function are introduced below [20–27]:

$$\mathrm{J(k)} = \sum_{\mathrm{i=1}}^{\mathrm{P}} \mathrm{Q}.[\hat{\mathrm{y}}(\mathrm{k+i|k}) - \mathrm{r(k+i|k)}]^2 + \sum_{\mathrm{i=0}}^{\mathrm{M-1}} \mathrm{R}.[\Delta\mathrm{u(k+i|k)}]^2 \tag{6}$$

Subject to

$$\mathrm{y_{min}} \leq \hat{\mathrm{y}}(\mathrm{k+i|k}) \leq \mathrm{y_{max}} \tag{7}$$

$$\mathrm{u_{min}} \leq \mathrm{u(k+i|k)} \leq \mathrm{u_{max}} \tag{8}$$

$$\Delta\mathrm{u_{min}} \leq \Delta\mathrm{u(k+i|k)} \leq \Delta\mathrm{u_{max}} \tag{9}$$

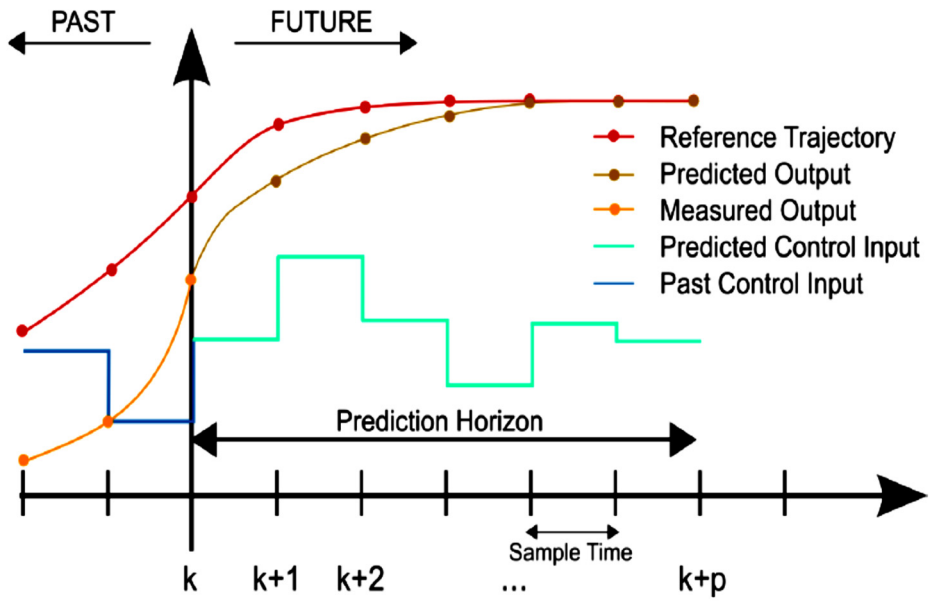

Figure 2. The MPC behavior at sampling instant t.

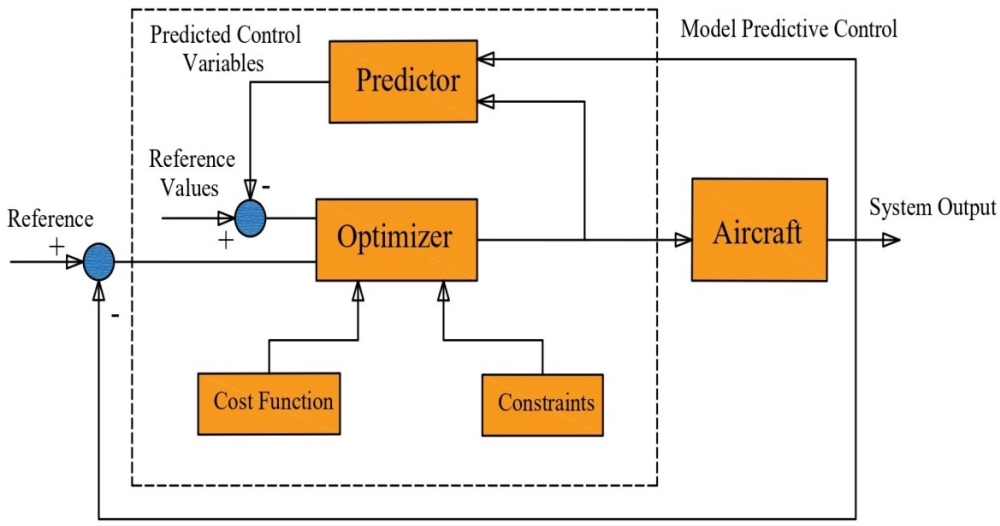

Figure 3. MPC flight control block diagram.

In the above Equations, the prediction horizon is symbolized as P and the control horizon as M. Discrete time as k, i is the indicator through the P interval, Q and R stand for output error weights and manipulated variable changing, respectively. In addition, $\hat{y}(k+i|k)$ and $r(k+i|k)$ represent output based prediction and command at time k+i, respectively. Besides, $u(k+i|k)$ and $\Delta u(k+i|k)$ are the best manipulated variable-based prediction and the manipulated variable forecasting rate at time k+i, respectively.

Model Flight Predictive Control

The proposed MPC controller will receive the signal of the pilot stick and set the point value of the pilot stick in inches as the system input, to represent the system control signal. Command values of the pilot stick are chosen to be step, multistep, and square signals. The MPC strategy is used to predict the control signal depending on the signal of the pilot stick and the set point value of the pilot stick in inches as a system input. The suggested control design is developedvia the MPC toolbox in Matlab. The creationof MPC is begun

by obtaining the linear time-invariant (LTI) system form of the aircraft application. The LTI form is represented by the state-space model as given in Equation (10).

$$A = \begin{bmatrix} -20 & 0 & 0 & 0 & 0 \\ -137.69 & -0.6571 & -0.00592 & 0 & 0 \\ -1280 & 689.4 & -0.6385 & 0 & 0 \\ 0 & 0 & 0.0014505 & -2.5259 & 0 \\ 0 & 1 & 0 & 0 & -4.144 \end{bmatrix}, B = \begin{bmatrix} 1 \\ 0 \\ 0 \\ 0 \\ 0 \end{bmatrix}$$
$$C = [0\ 0.8156\ 0\ 1.71\ -0.9567], \tag{10}$$

Taking into consideration a period of sampling time (Ts) and several applied control signals (N), the MPC methodology will operate at a certain rate equal to 1/N*Ts. It is very important to know that the choice of suitable Ts is very important since it calculates the length of the forecasting step. Furthermore, the behavior and accomplishment of the MPC are influenced inevitably by the choiceof P and M. In addition, there are two numerical weighting parameters, Q and R, that must be selected carefully for the system input and output, respectively. As a result, the BIA is used to get the best values of Ts, P, M, Q, and R.

This research concentrates on the tuning of MPC parameters for aircraft longitudinal flight control by applying the BIA. The main target of the optimization is to detect the optimal parameters of the MPC that enhance the damping characteristics ofthe aircraft system via decreasing the integral time absolute error (ITAE). The ITAE is given in the following equation,

$$\text{ITAE} = \int_0^\infty t|e(t)|dt \tag{11}$$

where **t** refers to time in seconds.

4. NARMA-L2 Control Strategy

The neuro-controller is represented by two various names: NARMA-L2 controller and feedback linearization controller [33]. The neuro-controller is called a feedback linearization controller when the model of the system has an attendant form. It is represented as a NARMA-L2 controller when the system model is formulated through the identical representation form. The main target of this control strategy is to convert the nonlinear plant into a linear dynamic model via canceling the nonlinearities [33,34].

As explained in the case of MPC, the first process in utilizing the NARMA-L2 controller is to choose the required model to be controlled. The neural network (NN) will be trained to characterize the system's forward dynamics. The first task is to choose a suitable structure forthe used model structure. The model of autoregressive-moving average (ARMA) is considered a common standard model to characterize the nonlinear system with discrete-time forms [35] as follows,

$$y(k+d) = N[y(k),\ y(k-1), \ldots,\ y(k-n+1),\ u(k),\ u(k-1), \ldots,\ u(k-n+1)] \tag{12}$$

where *u(k)* stands for the control signal, and *y(k)* represents the output of the system response. In the stage of system identification, the neural network is trained to estimate the nonlinear function '*N*'. Besides, the nonlinear strategy of control in the following form is used to help the output of the system to follow a trajectory of command reference '*y(k + d) = yr(k + d)*' [33–35].

$$u(k) = G[y(k),\ y(k-1), \ldots,\ y(k-n+1),\ y_r(k+d),\ u(k-1), \ldots,\ u(k-m+1)] \tag{13}$$

The main problem with applying the nonlinear controller in the above equation is that it is difficult to train the NN to obtain the function '*G*' to decrease the mean square error (MSE) because using a dynamic backpropagation will be quite slow. An approximate model is used to represent the system dynamics to solve the problem of using dynamic backpropa-

gation. The used controller is dependenton the NARMA-L2 simplified formulation [33–35] as follows,

$$\begin{aligned} y(k+d) &= f[y(k),\ y(k-1),\ldots,\ y(k-n+1),\ u(k-1),\ldots,\ u(k-m+1)] \\ &+g[y(k),\ y(k-1),\ldots,\ y(k-n+1),\ u(k-1),\ldots,\ u(k-m+1)]\ u(k) \end{aligned} \tag{14}$$

The shown formulation in the above equation is in companion form, where the next control strategy input *u(k)* is free from nonlinearity. The target of this representation is that the solving of the control signal makes the system response follow a certain reference, *y(k + d) = yr(k + d)*. The designed controller is formulated in Equation (15) [33–35].

$$u(k) = \frac{y_r(k+d) - f[y(k),\ y(k-1),\ldots,\ y(k-n+1),\ u(k-1),\ldots,\ u(k-n+1)]}{g[y(k),\ y(k-1),\ldots,\ y(k-n+1),\ u(k-1),\ldots,\ u(k-n+1)]} \tag{15}$$

Using this (15) directly can lead to realization issues because the control signal u(k) should be adjusted based on the system response (*k*) simultaneously. So, the defined formulation in the following equation can be used to overcome the realization problems.

$$\begin{aligned} y(k+d) &= f[y(k),\ y(k-1),\ldots,\ y(k-n+1),\ u(k),\ u(k-1),\ldots,\ u(k-n+1)] \\ &+g[y(k),\ldots,\ y(k-n+1),\ u(k),\ldots,\ u(k-n+1)]u(k+1) \end{aligned} \tag{16}$$

where $d \geq 2$. Figure 4 shows the structure of a neural networkscheme.

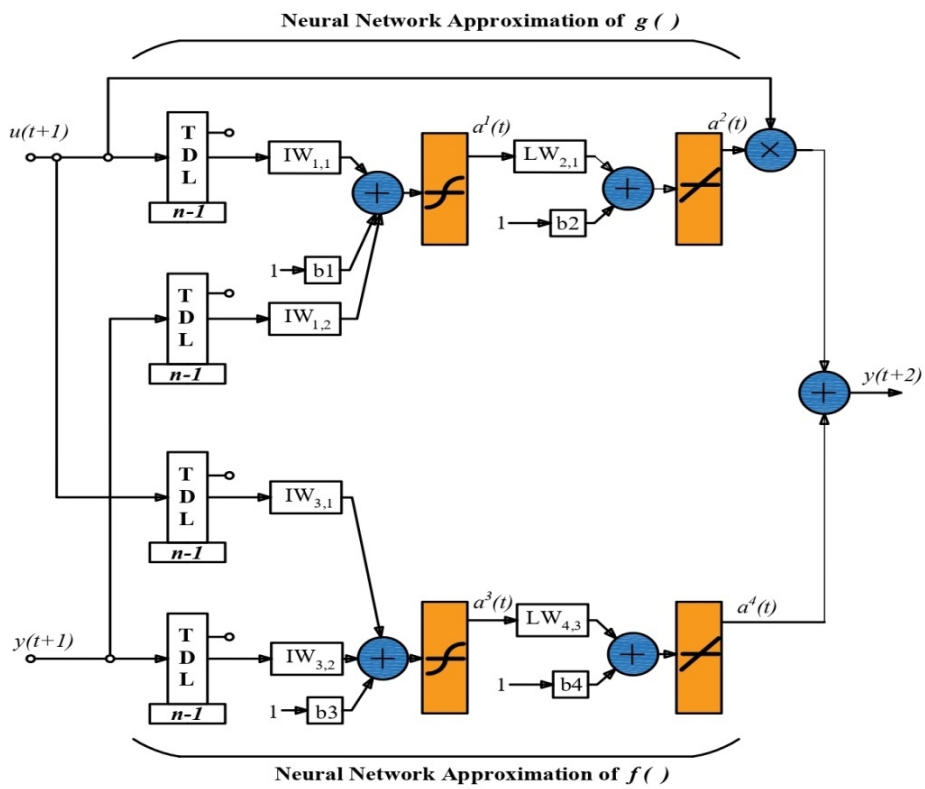

Figure 4. Neural Network Structure.

In the case of applying the model of NARMA-L2, the controller will introduce as in Equation (17) [33–35],

$$u(k+1) = \frac{y_r(k+d) - f[y(k),\ldots,\ y(k-n+1),\ u(k),\ldots,\ u(k-n+1)]}{g[y(k),\ldots,\ y(k-n+1),\ u(k),\ldots,\ u(k-n+1)]} \tag{17}$$

where the controller is convertible for d≥2. Figure 5 describes the schematic diagram of the NARMA-L2 controller.

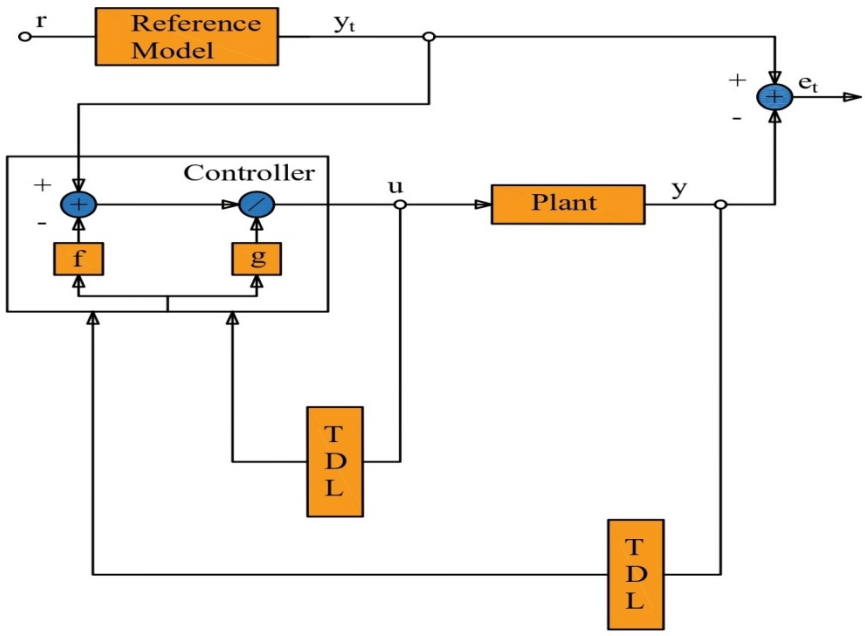

Figure 5. NARMA-L2 block diagram.

This control strategy is demonstrated with the above-described NARMA-L2 scheme, as presented in Figure 6 [33–35].

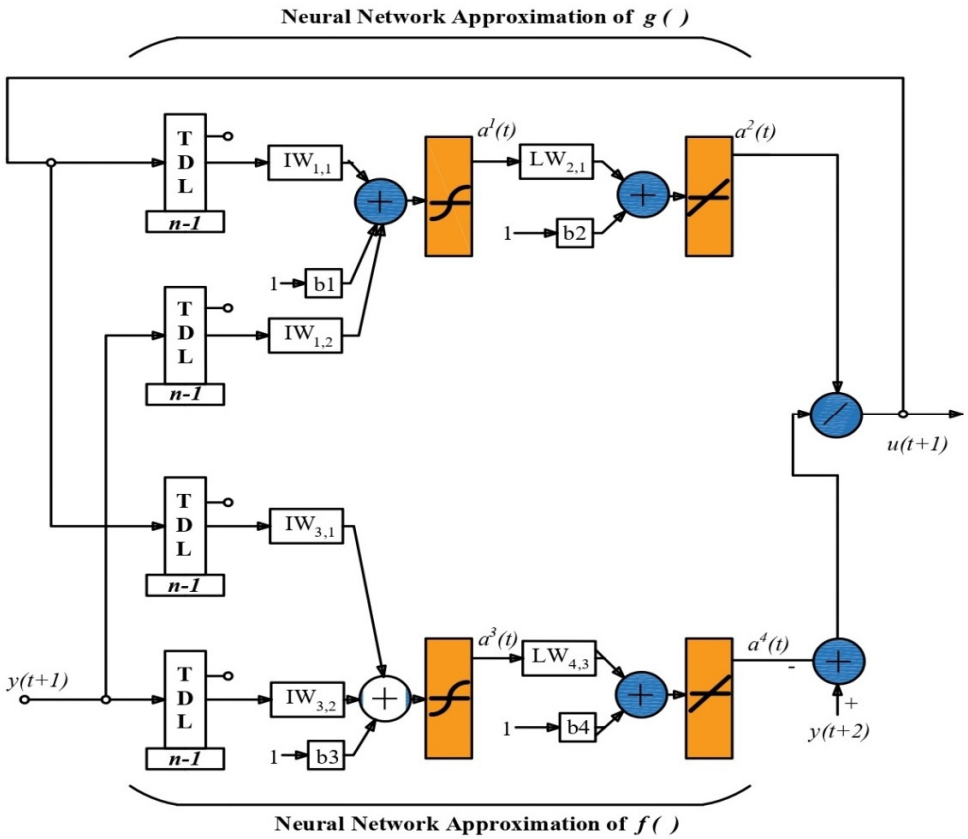

Figure 6. NARMA-L2 with the neural network model.

5. Bat Inspired Algorithm Overview

This paper suggested the BIA as a recent optimization algorithm that does notneed more adjustable factors. In addition, cooperation between multi-agents is utilized in the

BIA to enhance the exploration behavior that improves the global search and against the trapping problem in a certain local optimum position [36]. The bat-inspired algorithm has been expanded depending on the bats' manner for echolocation in findingtheir victims. The ideas of tuning based on BIA were firstly presented by Yang [36]. The bats generate continuous ultrasound pulses and then wait for listening to the echoes that rebound reverse from the adjacent targets. The gap inultrasound pulses changes based on the types and raises utilizing harmonics. The ultrasound waves reverberate with time delays and various levels of sound that allow each bat to take prey [37]. Naturally, virtual bats are used in the simulation process. Moreover, the displacementx_i and velocity v_i for every virtual bat are renewed through the process of optimization. The following equations represent the new displacements x_i^t and velocities v_i^t at time stage [36–38].

$$f_i = f_{min} + (f_{max} - f_{min})\beta \tag{18}$$

$$v_i^t = v_i^{t-1} + \left(x_i^t - x_*\right) f_i \tag{19}$$

$$x_i^t = x_i^{t-1} + v_i^t \tag{20}$$

where β stands for random factor obtained based on a function with uniform distribution and $\beta \in [0, 1]$. x_* is the current global best location derived after the arrangement process for all solutions/displacements among all n bats. Given that, the velocity is presented by $v_i = \delta_i f_i$. The velocity will be changed if there is an increase in either f_i or δ_i. To start the operation of the optimization process, each bat will randomly allocatea frequency $f_i \in [f_{min}, f_{max}]$. Intended for the local process search, a new solution/displacement for every bat is generated locally based on a random walk in case of selecting one solution between the current best locations/solutions [38].

$$x_{new} = x_{old} + \varepsilon K^t, \quad \varepsilon \in [-1, 1] \tag{21}$$

where ε is defined as a random number. In addition, K^t represents the average loudness of all bats at this time stage. In case a bat finds its prey, its loudness will be decreased, but the rate of its pulse generation grows and then loudness is chosen as any suitable value. The case of zero loudness demonstrates that the bat has presently found prey and temporarily stops transmitting every sound. This is adjusted through the below formulation [36–38]:

$$K_i^{t+1} = \alpha K_i^t 0 < \alpha < 1, \quad r_i^{t+1} - r_i^0 \left(1 - e^{-\gamma t}\right), \ \gamma > 0 \tag{22}$$

where r_i is the pulse emission rate of bats. As the final iteration is reached, zero loudness is achieved, and $\gamma_i^t = \gamma_i^0$.

The tuning cycle of MPC parameters is shown in Figure 7. The BIA takes the error as in Equation (11) as the objective function to be minimized, then tunes the parameters.

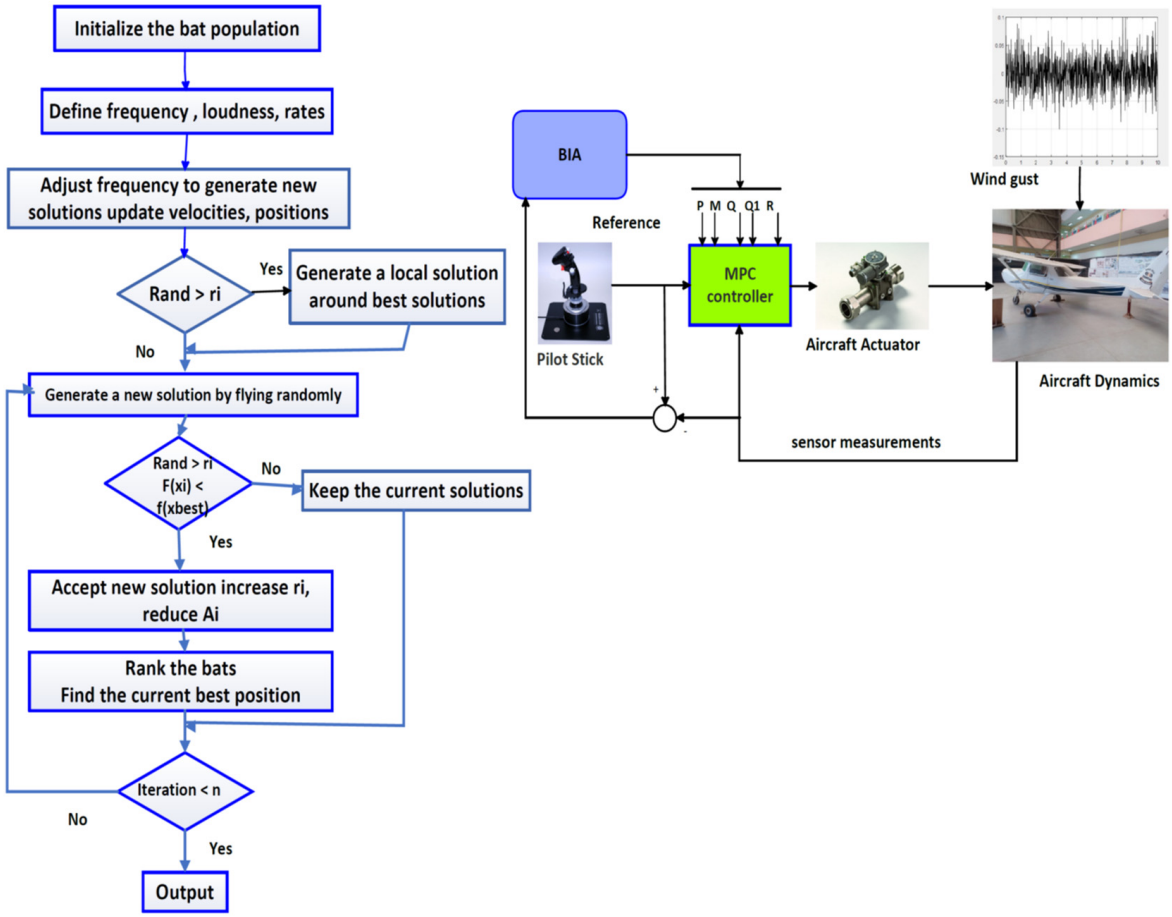

Figure 7. The BIA flowchart with aircraft model predictive controller tuning process.

6. Results and Discussions

In this research, simulation processes were carried out based on the traditional PI controller, NARMA-L2 controller, and the proposed BIA-based MPC controller for a longitudinal motion of aircraft flight system when using step, square and multistep signals for the aircraft pilot stick. Table 1 records the best values of the controller parameters and corresponding values of the performance index (ITAE) and cross-correlation function (XCF). As in Table 1, the recommended BIA-based MPC strategy has the best damping characteristics and the minimum ITAE and XCF values compared with the traditional PI controller and NARMA-L2 controller.

Identification results of the NARMA-L2 aircraft model: The identification of the aircraft model is obtained based on 10,000 samples of input/output data that are collected from the original system model. A random input signal, $u_k[-1,1]$ is used to excite the aircraft system to collect the dataset that is used in the identification process. The collected datasets are split into three parts:the training dataset is utilized to train the model of NARMA-L2, the validation dataset is intended to validate the obtained model, and the testing dataset is utilized to test the generated aircraft neural model.

With the aim of training the neural network, which arranged the NARMA-L2 established model, the initial biases and weights are unsystematically chosen. The mean squared error (MSE) for the target error is selected to be 10^{-7}. The optimal structure of the neural network is built dependingon heuristics, which achieves the least MSE after utilizing various numbers of hidden layer neurons for the ANN. The Levenberg Marquardt is used as an optimization routine for the learning process in the neural network model. The number of epochs for training is 500 iterations. The training, validation, and testing data are shown in Figures 8–10, respectively. These figures present the excitation input,

plant output, NN output, and error.It is clear from the figures that the error is negligible and close to zero for all the tests which demonstrates a strong significance that the NN model is agreeable.

Table 1. The optimum value of controller parameters and performance criteria.

		Conventional PI	NARMA-L2	BIA Based MPC
Controller parameters		$K_p = -1.746$, $K_i = -3.864$	It is defined in Figure 9	$Ts = 0.01$, $P = 11$, $M = 1$, $Q = 1.4024$, $R = 0.22449$
Step	performance	$T_r = 0.24$ s, $T_s = 2.26$ s, %O.S = 0.8385%, Peak: 1.008	$T_r = 0.19$ s, $T_s = 10$ s, %O.S = 0.8854%, Peak: 1.009	$T_r = 0.25$ s, $T_s = 0.46$ s, %O.S = 0.44%, Peak: 1.002
	ITAE	0.161	0.7	0.105
Multistep	ITAE	75.05	444.1	39.1
	XCF (%)	94.43	88.63	95.44
Square	ITAE	49.74	18.87	25.23
	XCF (%)	94.93	98.1	95.94

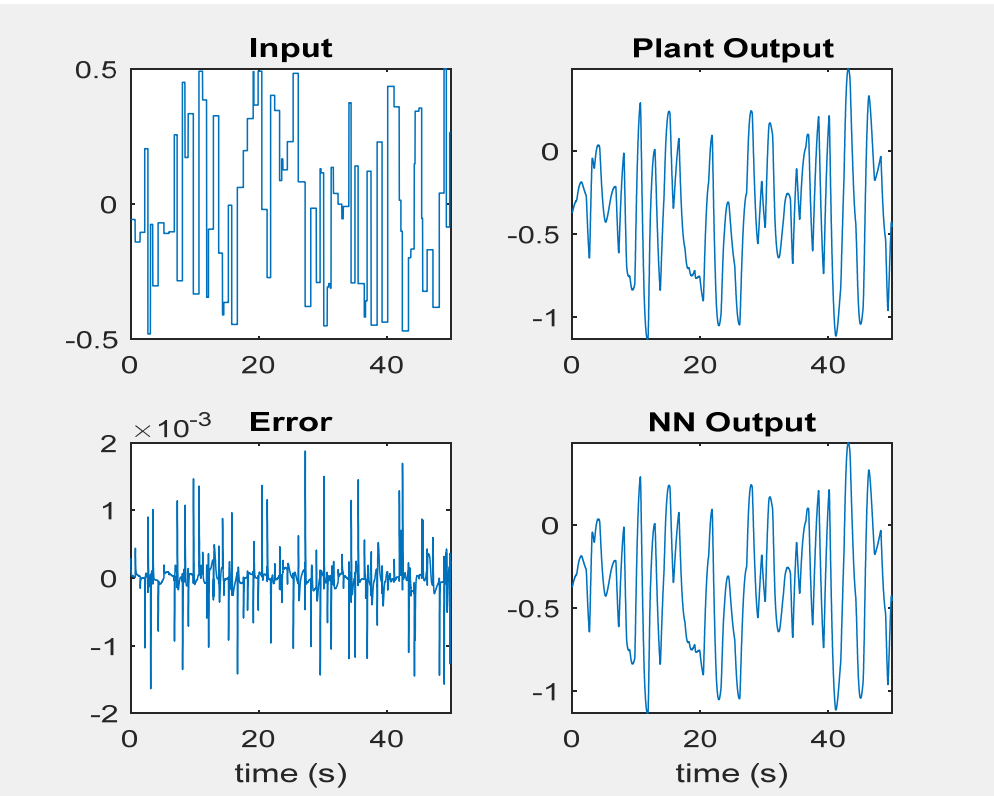

Figure 8. Training data of neural network.

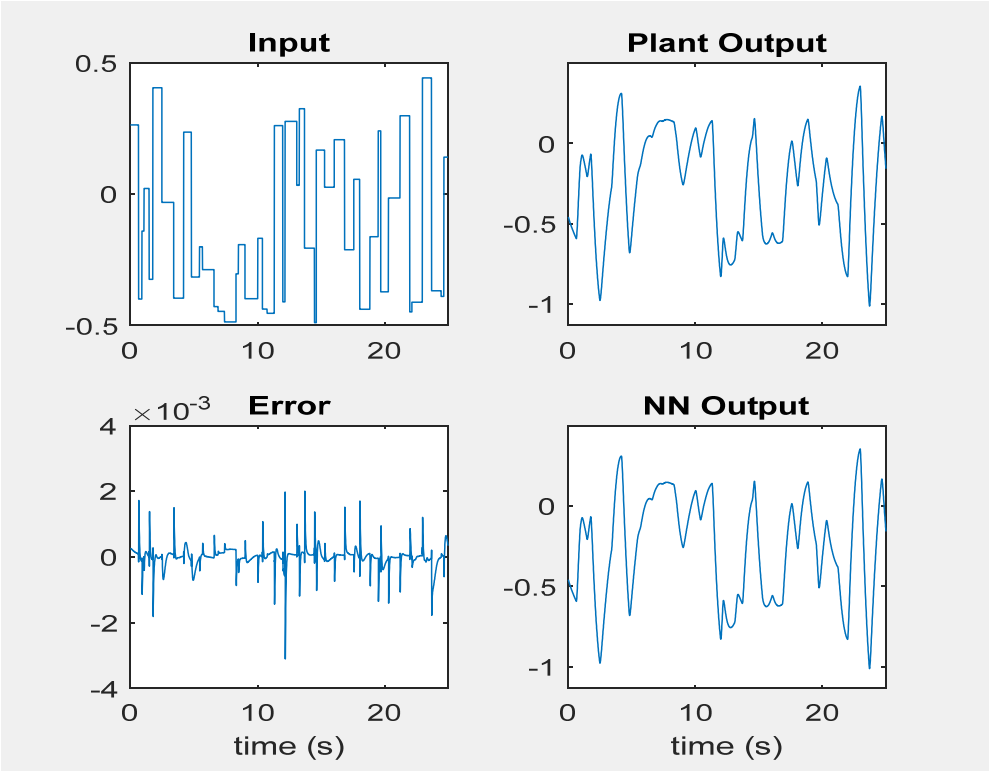

Figure 9. Validation data of neural network.

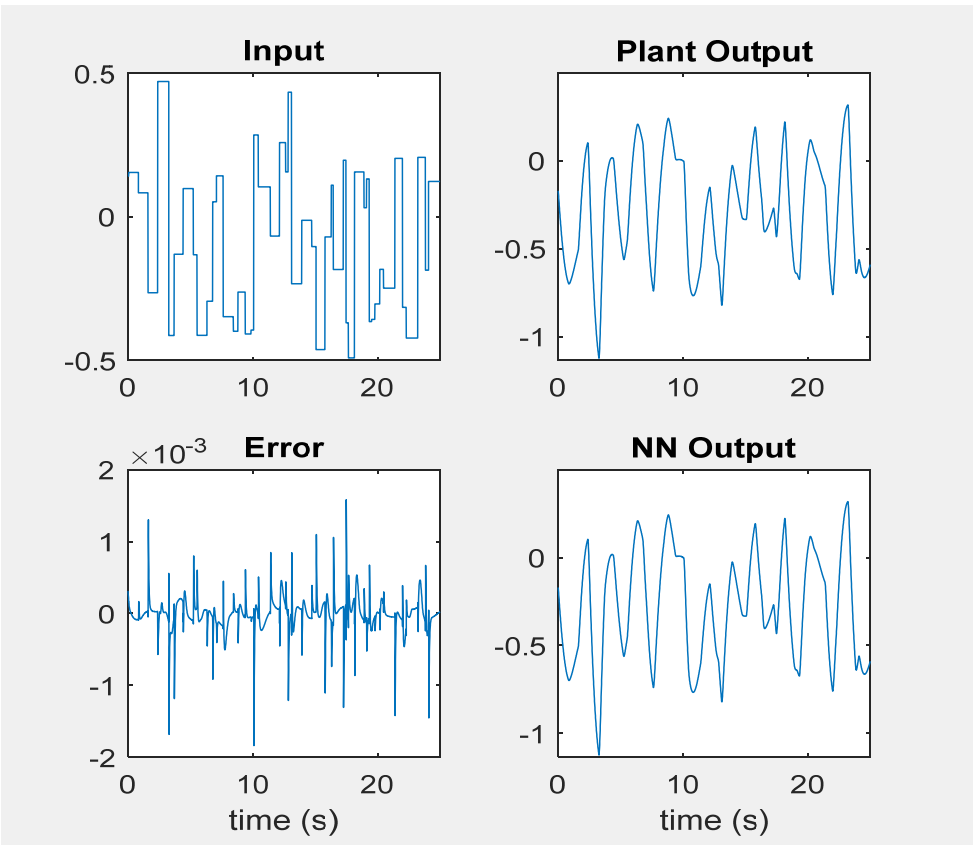

Figure 10. Testing data of neural network.

After designing the proposed BIA-based MPC, the traditional PI controller, and NARMA-L2 controller, the following test scenarios are produced to check the effectiveness of the proposed controller at the nominal case, system parameters perturbation, and disturbance.

6.1. Nominal Case

To evaluate the effectiveness and the performance of the suggested control strategies, the controller is used to adjust the longitudinal movement of aircraft as flight control. Three different signals of trajectory control are applied to the model namely step, multistep and square signals. These signals are applied to the system based on PI, NARMA-L2, and BIA-based MPC controllers. The performance criteria including settling time, overshoot, rise time, ITAE, XCF, and peak response for the suggested control strategies are presented in the chart plots in Figures 11 and 12. In addition, the simulation responses are shown in Figures 13–18. Considering the results in Table 1, the proposed BIA-based MPC demonstrates an acceptable result witha settling time of about 0.46 sec, an overshoot of about 0.44%, and an ITAE of about 0.106 in comparison with traditional PI and NARMA-L2 controllers. Figures 13 and 14 clarify the effectiveness of the proposed controller which confirms the numerical results in Table 1. In Figure 12, the NARMA L2 gives an oscillation in the system response and it is very clear inthe zoomed part in Figures 13 and 14.

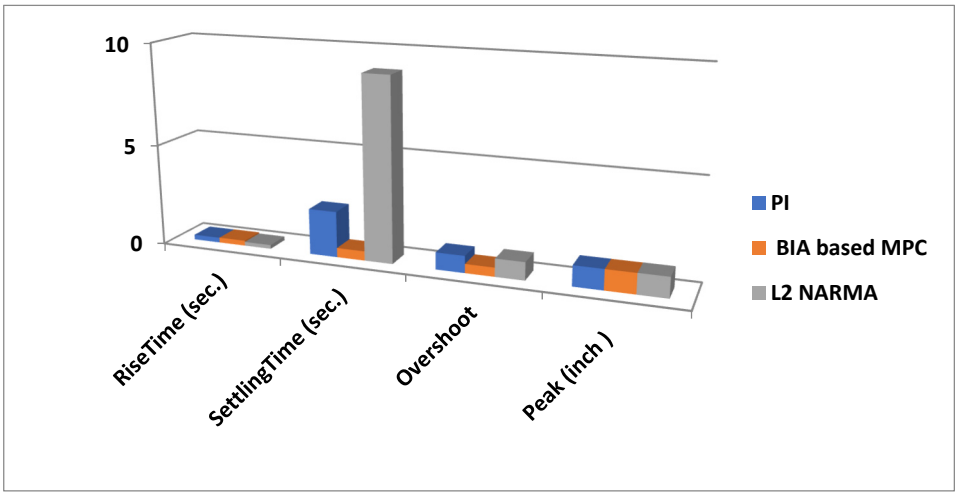

Figure 11. Chart of performance criteria in the nominal case.

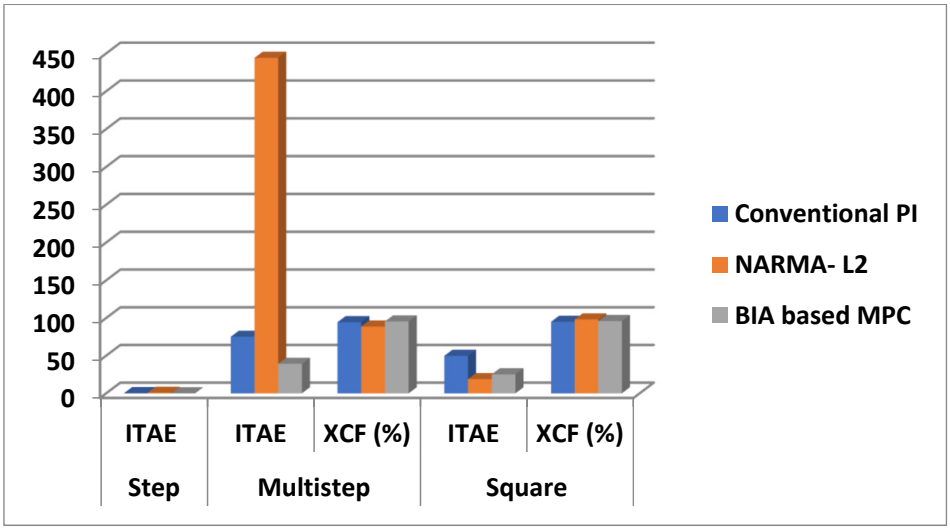

Figure 12. Chart of ITAE and XCF in the nominal case.

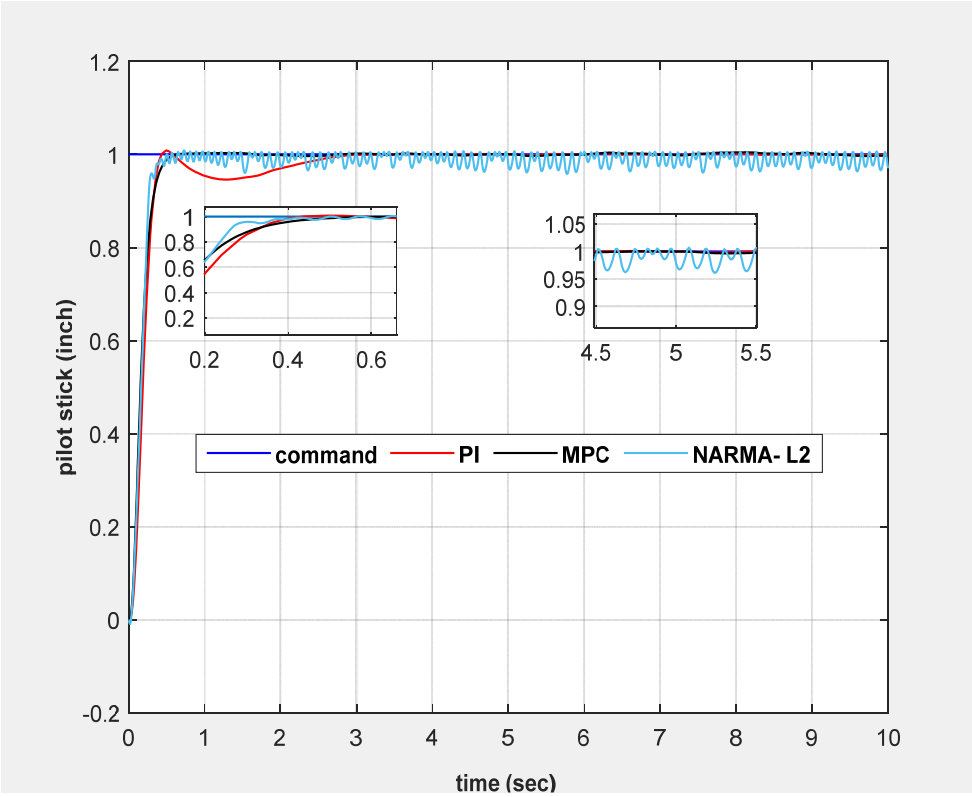

Figure 13. Pilot stick step response.

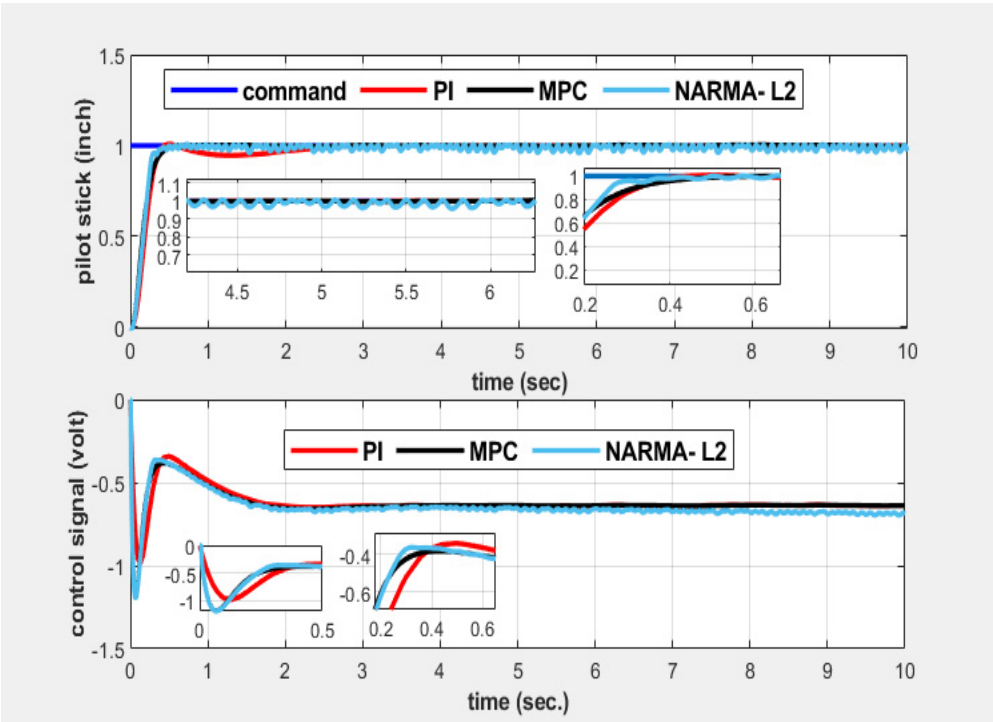

Figure 14. Pilot stick step response with corresponding error.

6.2. System Parameters Perturbationand Disturbance case

It is very important to attest to the robustness of the recommendedBIA-based MPC control methodology. For this requirement, deviations in the parameters of the aircraft model and operating points conditions are taken into the account. Figures 15 and 16 show

the change in input profile as multi-amplitude and multi-frequency signals to check the system robustness against strong variations in the input signal. In addition, the system input signal is changed to be a square wave as given in Figures 17 and 18. Considering Figures 15–18, it is very obvious that the BIA-based MPC introduces better tracking control compared to the PI controller and the NARMA-L2 controller which gives an oscillation output response. In addition, in Table 1, two different performance indices including cross-correlation function (XCF) and ITAE are used to evaluate the tracking performance for the suggested controllers. The numerical data in Table 1 arepresented in the chart plot as given in Figure 12. In this situation, the BIA-based MPC demonstrates acceptable numerical results for the pilot stick control tracking based on multistep and square command inputs. Figures 19–21 demonstrate the system performance in case of system variations by 20%, 30%, and 40%. Moreover, Figures 22–24 demonstrate the system response based on the PI, NARMA-L2, and BIA-based MPC, respectively, with variations in the actuator coefficient (T_a) by 20%, 30%, and 40%. Table 2 demonstrates the performance criteria for the proposed controller in the case of system perturbation. From this simulation result and considering numerical results in Table 2, it is observed that the aircraft modelis stable with the suggested BIA-based MPC controller compared with other controllers. Furthermore, the investigated MPCs control methodologies have the capability to extinguish the system oscillations under parameter deviations and variations in contrast with NARMA-L2 and PI controllers.

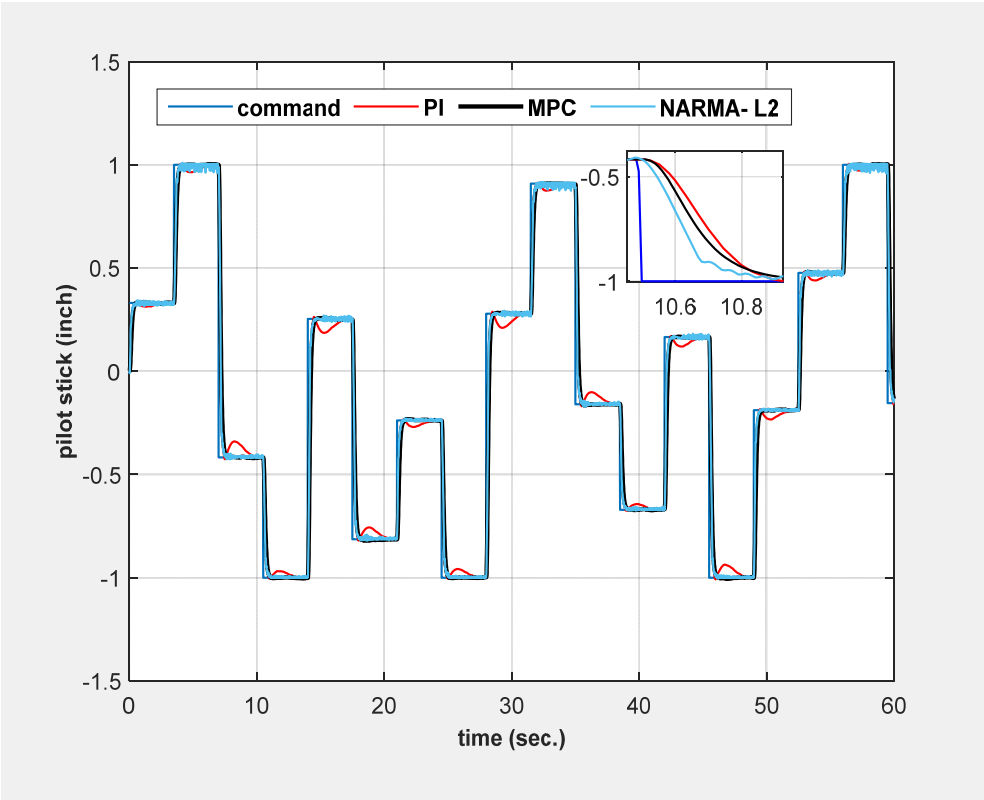

Figure 15. Pilot stick multistep response without corresponding error.

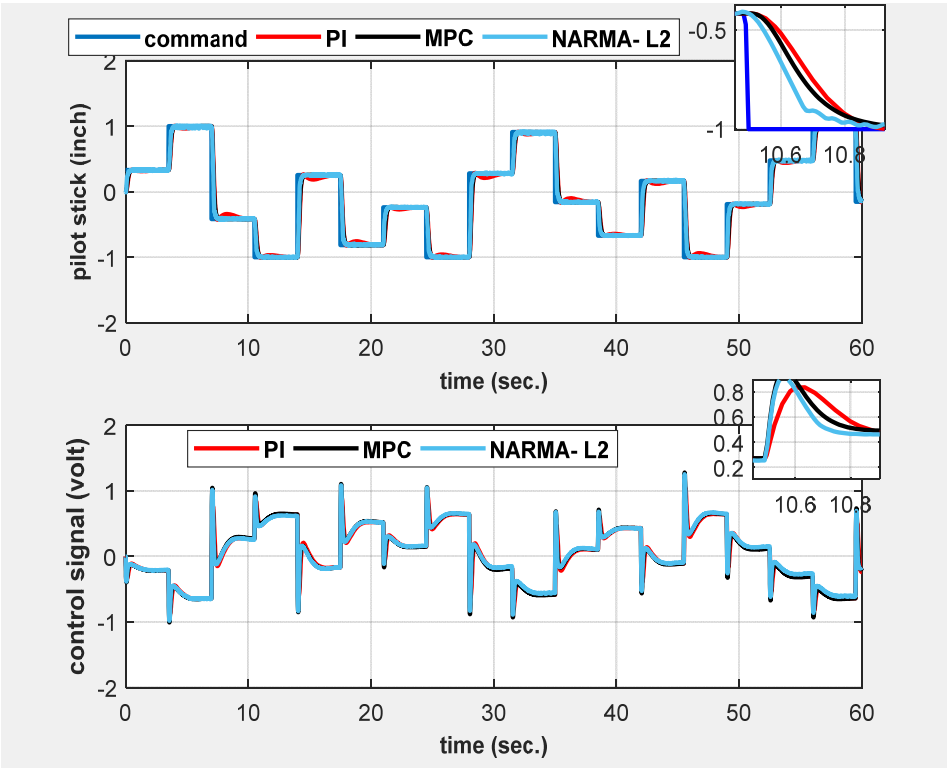

Figure 16. Pilot stick multistep response with corresponding error.

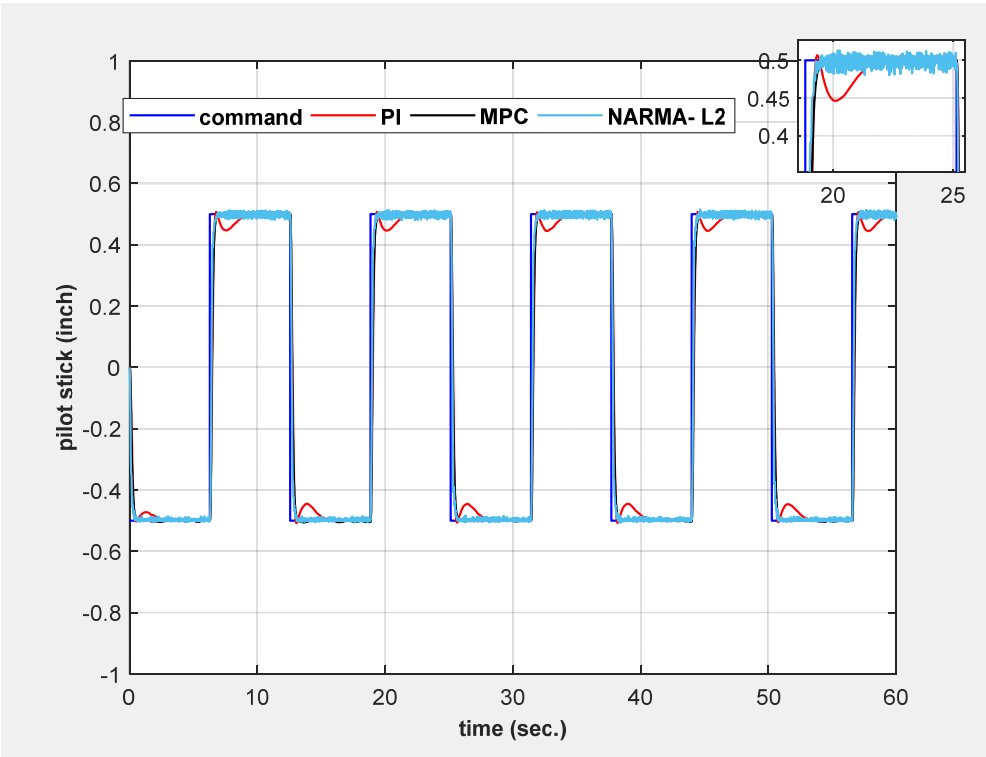

Figure 17. Pilot stick square wave response.

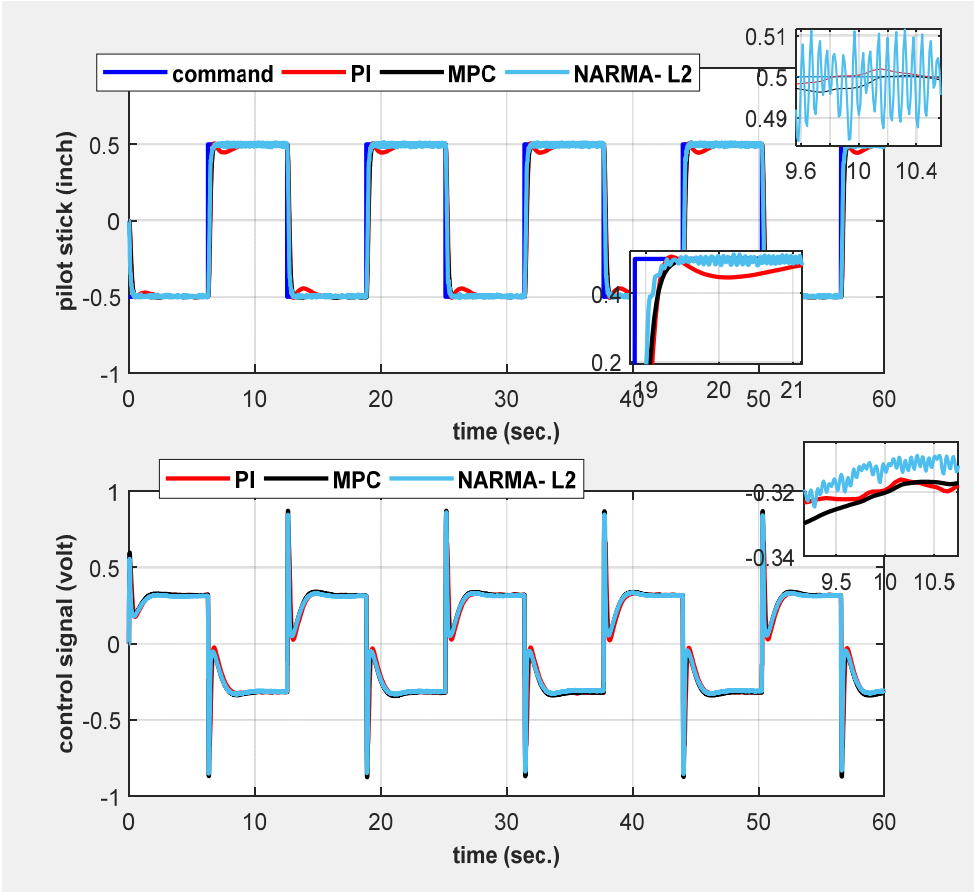

Figure 18. Pilot stick square wave response with corresponding error.

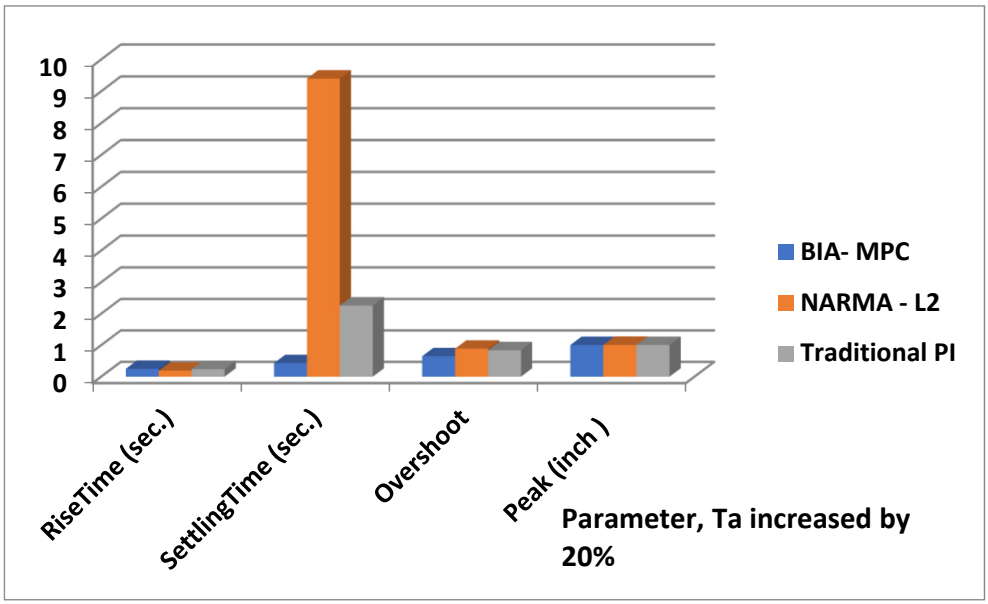

Figure 19. Chart of performance criteria in system perturbation by 20%.

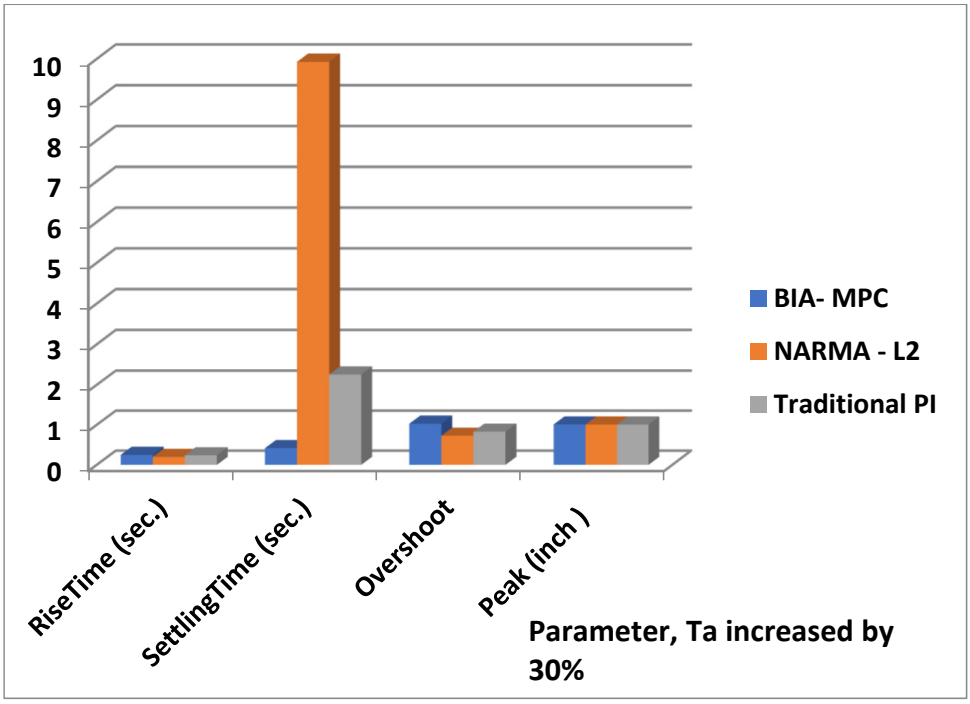

Figure 20. Chart of performance criteria in system perturbation by 30%.

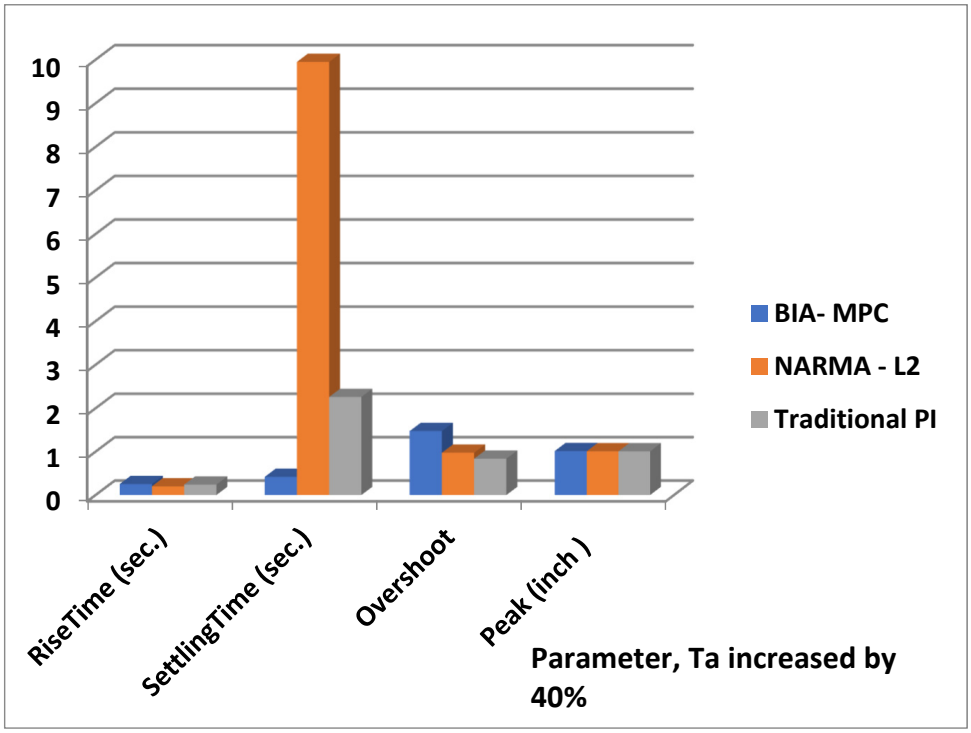

Figure 21. Chart of performance criteria in system perturbation by 40%.

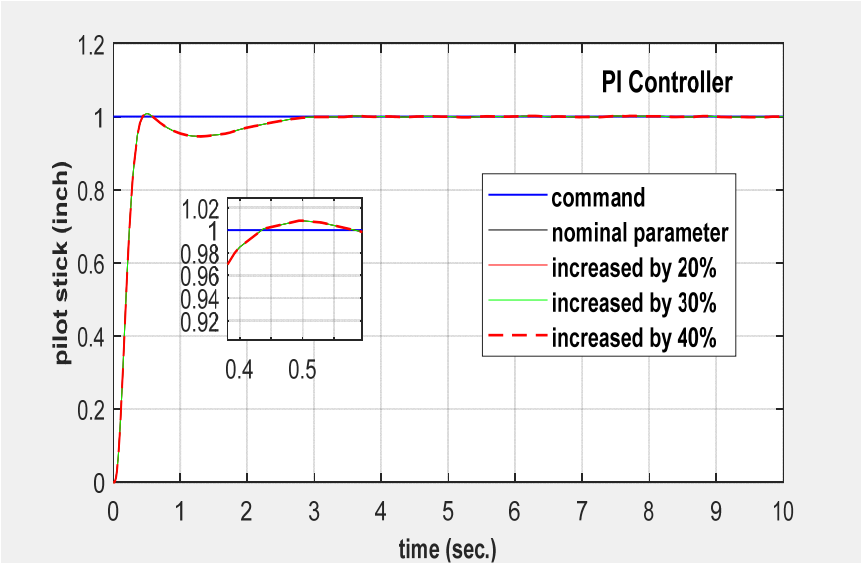

Figure 22. System response based PI with parameters perturbation.

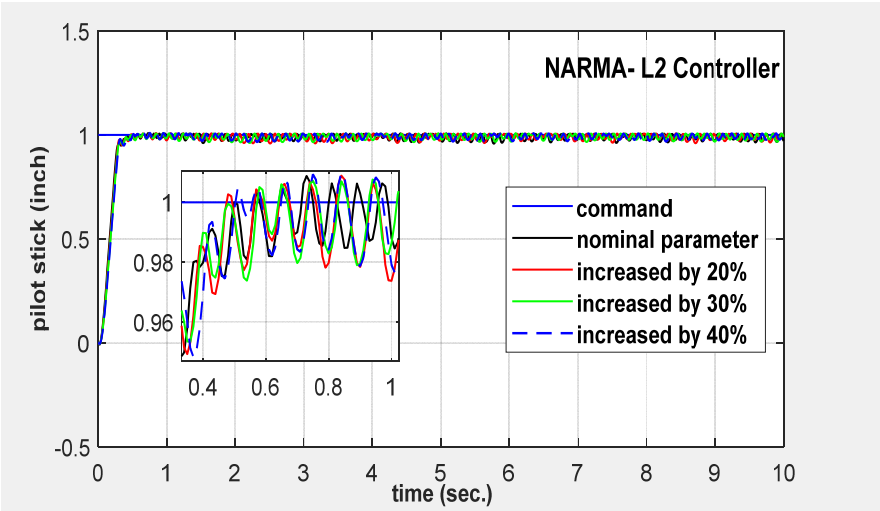

Figure 23. System response basedNARMA-L2 with parameters perturbation.

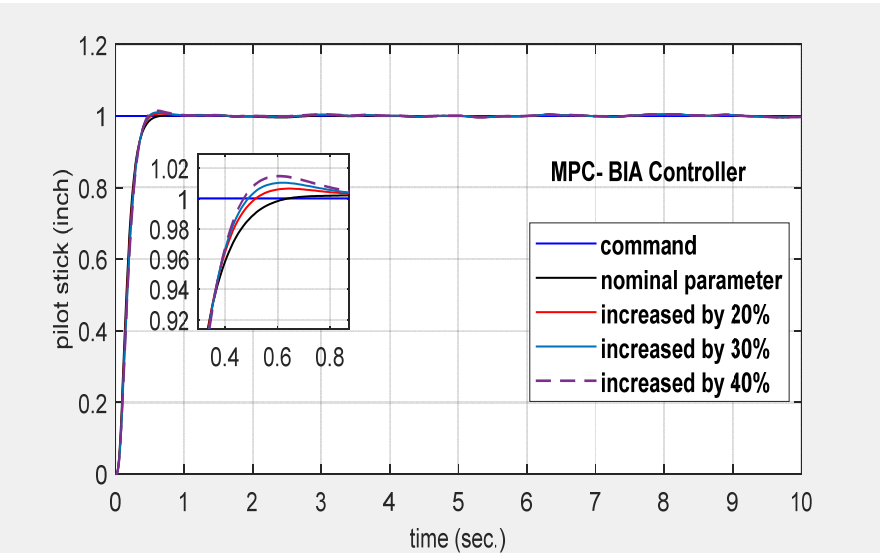

Figure 24. System response based MPC-BIA with parameters perturbation.

Table 2. Evaluation of Controllers Based on System Parameter Perturbation.

Type of Controller	Perturbations	RiseTime (s)	SettlingTime (s)	Overshoot (%)	Peak (inch)
BIA-MPC	nominal	0.2504	0.4612	0.4465	1.0045
NARMA-L2		0.19	9.5	0.8854	1.0089
Traditional PI		0.24	2.26	0.838	1.0084
BIA-MPC	20%	0.25	0.43	0.65	1.006
NARMA-L2		0.19	9.4	0.89	1.0089
Traditional PI		0.24	2.26	0.838	1.008
BIA-MPC	30%	0.25	0.42	1.03	1.0104
NARMA-L2		0.2	9.93	0.727	1.0078
Traditional PI		0.24	2.26	0.83	1.008
BIA-MPC	40%	0.254	0.419	1.475	1.0147
NARMA-L2		0.202	9.95	0.975	1.0098
Traditional PI		0.24	2.26	0.838	1.008

To study the system robustness, a disturbance signal has been added to the control signal of the actuator as shown in Figure 25. The system response based on the disturbance signal is given in Figure 26. The BIA-based MPC still maintains its robustness and high performance for tracing the pilot stick input for the flight control system. In addition, NARMA-L2 cannot damp the system oscillatory and it is more increased compared tothe nominal case study, making the system more unstable. Finally, the numerical and graphical results give the leading of BIA-based MPC to regulate the longitudinal movement of aircraft. In addition, it can be summarized that the NARMA-L2 regulator is supposedly powerful and it presents a satisfactory system modeling-based neural network. However, it introduces poor response in the aircraft motion control of longitudinal behavior. This complies with the cleared chattering in the output aircraft response.

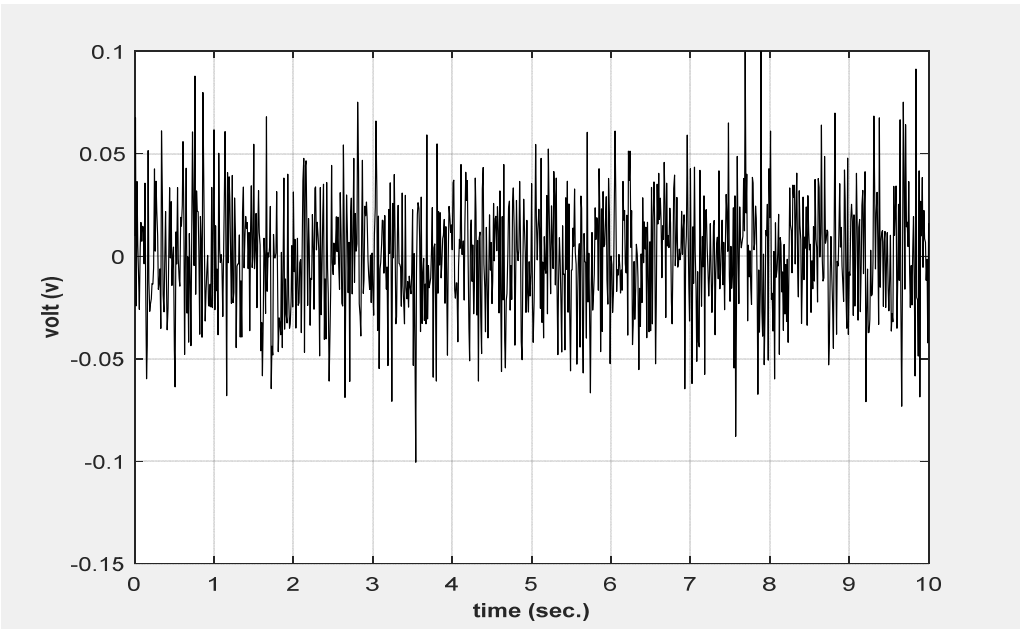

Figure 25. Disturbance signal.

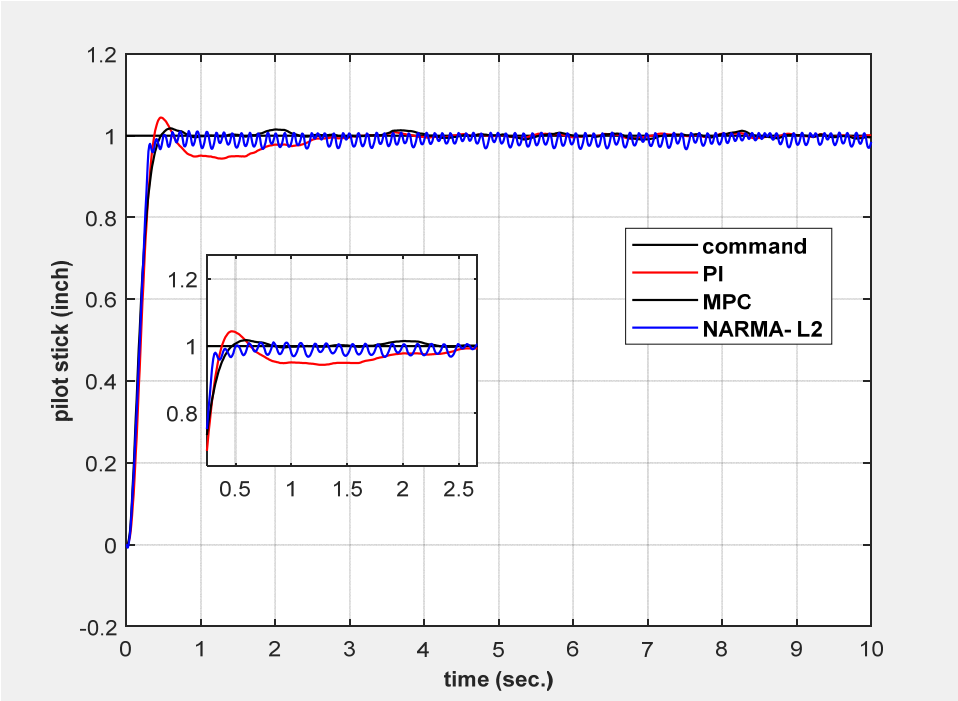

Figure 26. System response based controllers with disturbance.

7. Conclusions

This paper introduces a new intelligent tuning for the model predictive longitudinal motion flight controller based on a new algorithm named BIA. The BIA algorithm is used to find the best parameters of the MPC rather than the trial and error or designer experience. A defined ITAE-based performance index has been used to decrease both settling time and maximum overshooting simultaneously. Besides, the longitudinal motion of aircraft control is carried out based on the NARMA-L2 controller to evaluate the accomplishment of the suggested MPC based on BIA.Despite the spreading fact that the NARMA-L2 control strategy introduces an inspiring method to precisely control the nonlinear system, this paper revealed that this controller has a high chattering, as seen from the simulation result responses of the longitudinal motion of aircraft flight control at different desired profile trajectories. Evaluating the suggested BIA-based MPC with the traditional PI and NARMA-L2 controllers proved the superiority of the developed BIA-based MPC to track the system reference with distinct results forsettling time, maximum overshoot, and ITAE. Furthermore, the suggested BIA-based MPC can guarantee the stability of the aircraft system under system perturbation and system disturbance that can be established forvarious engineering applications in future work.

Author Contributions: Conceptualization, M.S.E., M.F.A. and A.M.E.; methodology, M.E.-S.M.E. and M.E.; software, A.M.E.; validation, M.E.-S.M.E., M.E. and A.M.E.; formal analysis, M.S.E.; investigation, M.E.-S.M.E. and M.E.; resources, M.F.A.; data curation, M.E.; writing—original draft preparation, M.E.-S.M.E.; writing—review and editing, M.E.-S.M.E. and M.E.; visualization, M.E.-S.M.E., M.S.E. and M.F.A.; supervision, M.E.-S.M.E.; project administration, M.E. All authors have read and agreed to the published version of the manuscript.

Funding: This research received no external funding.

Institutional Review Board Statement: Not applicable.

Informed Consent Statement: Not applicable.

Data Availability Statement: Not applicable.

Conflicts of Interest: The authors declare no conflict of interest.

References

1. Pratt, R.W. *Flight Control Systems*; American Institute of Aeronautics and Astronautics: Reston, VA, USA, 2000.
2. Stengel, R.F. *Flight Dynamics*; Princeton University Press: Princeton, NJ, USA, 2015.
3. Murayama, M.; Togashi, F.; Nakahashi, K.; Matsushima, K.; Kato, T. Simulation of aircraft response to control surface deflection using unstructured dynamic grids. *J. Aircr.* **2005**, *42*, 340–346. [CrossRef]
4. Ahmed, W.; Li, Z.; Istan, M.; Anwar, M.B. Multi-objective Eigen structure Assignment-PID Based Controller Design for Longitudinal Motion of Aircraft. In Proceedings of the 2019 5th International Conferenceon Control Science and Systems Engineering (ICCSSE), Shanghai, China, 14–16 August 2019; pp. 40–44.
5. Kudryavtseva, I.; Efremov, A.; Panteleev, A. Optimization of helicopter motion control based on the aggregated interpolation model. In *AIP Conference Proceedings*; AIP Publishing LLC: Melville, NY, USA, 2019; Volume 2181, p. 020008.
6. Oktay, T.; Coban, S. Simultaneous longitudinal and lateral flight control systems design for both passive and active morphing TUAVs. *Elektron. Ir Elektrotechnika* **2017**, *23*, 15–20. [CrossRef]
7. Liu, S.; Yan, B.; Dai, P.; Xing, M. Morphing Aircraft Control Method Based on TS Fuzzy Control. In Proceedings of the 2019 IEEE 4th International Conference on Image, Vision and Computing (ICIVC), Xiamen, China, 5–7 July 2019; pp. 617–621.
8. Nair, M.P.; Harikumar, R. Longitudinal dynamics control of UAV. In Proceedings of the 2015 International Conference on Control Communication & Computing India (ICCC), Trivandrum, India, 19–21 November 2015; pp. 30–35.
9. Lin, P.N.W.; Nang, L.K.; Hla, M. Longitudinal and Lateral Dynamic System Modelling of a Fixed Wing UAV. *Int. J. Sci. Technol. Res.* **2015**, *4*, 171–174.
10. Ramya, R. PID Controller Design for Dynamic Motion of an Aircraft. In Proceedings of the Second International Conference on Emerging Trends in Science & Technologies For Engineering Systems (ICETSE-2019), Karnataka, India, 10–11 July 2019.
11. Iskrenovic-Momcilovic, O. Slidingmodecontrolforlongitudinalaircraftdynamics. *J. Autom. Mob. Robot. Intell. Syst.* **2018**, *12*, 55–60.
12. Hušek, P.; Narenathreyas, K. Aircraft longitudinal motion control based on Takagi–Sugeno fuzzy model. *Appl. Soft Comput.* **2016**, *49*, 269–278. [CrossRef]
13. Narenathreyas, K.B. Fuzzy Logic Control for Aircraft Longitudinal Motion. Master Thesis, Czech Technical University, Prague, Czech Republic, 2013.
14. Deepa, S.N.; Sudha, G. Longitudinal control of an aircraft using artificial intelligence. *Int. J. Eng. Technol. (IJET)* **2014**, *5*, 4752–4760.
15. Deepa, S.N.; Sudha, G. A design of longitudinal control of an aircraft using a fuzzy logic based PID controller. In *Proceedings of the Third International Conference on Soft Computing for Problem Solving*; Springer: New Delhi, India, 2014; pp. 547–559.
16. Harris, J.; Arthurs, F.; Henrickson, J.V.; Valasek, J. Aircraft system identification using artificial neural networks with flight test data. In Proceedings of the 2016 International Conference on Unmanned Aircraft Systems (ICUAS), Arlington, VA, USA, 7–10 June 2016; pp. 679–688.
17. Necsulescu, D.; Jiang, Y.W.; Kim, B. Neural network based feedback linearization control of an unmanned aerial vehicle. *Int. J. Autom. Comput.* **2007**, *4*, 71–79. [CrossRef]
18. Mjahed, M. Flight control system design using neural networks. *Int. Rob. Auto J.* **2019**, *5*, 96–99. [CrossRef]
19. Remple, R.K.; Tischler, M.B. *Aircraft and Rotor Craft System Identification: Engineering Methods with Flight-Test Examples*; American Institute of Aeronautics and Astronautics: Reston, VA, USA, 2006.
20. Essa, M.E.S.M.; Aboelela, M.A.; Moustafa Hassan, M.A.; Abdrabbo, S.M. Model predictive force control of hardware implementation for electro-hydraulic servo system. *Trans. Inst. Meas. Control.* **2019**, *41*, 1435–1446. [CrossRef]
21. Essa, M.E.S.M.; Aboelela, M.A.; Hassan, M.M.; Abdrabbo, S.M. Hardware in the loop of position tracking control of hydraulic servo mechanism. In Proceedings of the 2017 13th International Computer Engineering Conference (ICENCO), Cairo, Egypt, 27–28 December 2017; pp. 160–165.
22. Franko, S.; Koç, İ.M.; Özsoy, C.; Sari, N. Mpc and lqr type controller design and comparison for an unmanned helicopter. In Proceedings of the 2011 Summer Computer Simulation Conference, Hague, The Netherlands, 27–30 June 2011; pp. 138–144.
23. Meola, D.; Gambino, G.; Palmieri, G.; Glielmo, L. A comparison between LTV-MPC and LQR yaw rate-side slip controller. *IFAC Proc. Vol.* **2009**, *42*, 154–159. [CrossRef]
24. Elsisi, M. Optimal design of nonlinear model predictive controller based on new modified multitracker optimization algorithm. *Int. J. Intell. Syst.* **2020**, *35*, 1857–1878. [CrossRef]
25. Elsisi, M.; Ebrahim, M.A. Optimal design of low computational burden model predictive control based on SSDA towards autonomous vehicle under vision dynamics. *Int. J. Intell. Syst.* **2021**, *36*, 6968–6987. [CrossRef]
26. Elsisi, M.; Aboelela, M.; Soliman, M.; Mansour, W. Design of Optimal Model Predictive Controller for LFC of Nonlinear Multi-area Power System with Energy Storage Devices. *Electr. Power Compon. Syst.* **2018**, *46*, 1300–1311. [CrossRef]
27. Essa, M.E.S.M. Identification and Temperature Control for Thermal Model of a House Based on Model Predictive Control Tuned by Cuckoo Search Algorithm. In Proceedings of the 2019 15th International Computer Engineering Conference (ICENCO), Giza, Egypt, 29–30 December 2019; pp. 144–149.
28. Essa, M.E.S.M.; Aboelela, M.A.; Moustafa Hassan, M.A.; Abdrabbo, S.M. Design of model predictive force control for hydraulic servo system based on cuckoo search and genetic algorithms. *Proc. Inst. Mech. Eng. Part I J. Syst. Control. Eng.* **2020**, *234*, 701–714. [CrossRef]
29. El-Sayed, B.E.S.M.; Essa, M.E.S.M.; El-Beltagy, M.D. Modeling and Control of Aircraft Pilot Stick Based on Anfis Cuckoo Search Algorithm and System Identification. *J. Fract. Calc. Appl.* **2021**, *12*, 1–10.

30. Faraj, M.A.; Abbood, A.M. Fractional order PID controller tuned by bat algorithm for robot trajectory control. *Indones. J. Electr. Eng. Comput. Sci.* **2021**, *21*, 74–83. [CrossRef]
31. Singh, C.; Padhy, P.K. Fractional Order Controller Design for interconnected Power System using BAT optimization Algorithm. In Proceedings of the 2022 Second International Conference on Artificial Intelligence and Smart Energy (ICAIS), Coimbatore, India, 23–25 February 2022; pp. 1634–1639.
32. Yuvapriya, T.; Lakshmi, P.; Elumalai, V.K. Experimental Validation of LQR Weight Optimization Using Bat Algorithm Applied to Vibration Control of Vehicle Suspension System. *IETE J. Res.* **2022**, 1–11. [CrossRef]
33. Mokr, I.S.S.; Shafie, A. A Real time implementation of NARMA L2 feedback linearization and smoothed NARMA L2 controls of a single link manipulator. In Proceedings of the 2008 International Conference on Computer and Communication Engineering, Kuala Lumpur, Malaysia, 13–15 May 2008; pp. 691–697.
34. Çelikel, R. Speed control of BLDC using NARMA-L2 controller in single link manipulator. *Balk. J. Electr. Comput. Eng.* **2019**, *7*, 143–148. [CrossRef]
35. Adaryani, M.R.; Afrakhte, H. NARMA-L2 controller for three-area load frequency control. In Proceedings of the 2011 19th Iranian Conference on Electrical Engineering, Tehran, Iran, 17–19 May 2011; pp. 1–6.
36. Xin-She, Y. *A New Metaheuristic Bat-inspired Algorithm. Nature Inspired Cooperative Strategies for Optimization (NICSO 2010)*; Springer: Berlin/Heidelberg, Germany, 2010; pp. 65–74.
37. Kumar, P.; Narayan, S. Multi-objective bat algorithm tuned optimal FOPID controller for robust aircraft pitch control. *Int. J. Syst. Control. Commun.* **2017**, *8*, 348–362. [CrossRef]
38. Elsisi, M.; Soliman, M.; Aboelela, M.A.S.; Mansour, W. Optimal design of model predictive control with superconducting magnetic energy storage for load frequency control of nonlinear hydrothermal power system using bat inspired algorithm. *J. Energy Storage* **2017**, *12*, 311–318. [CrossRef]